Chemical Engineering Journal 299 (2016) 209–216

Contents lists available at ScienceDirect

Chemical Engineering Journal

journal homepage: www.elsevier.com/locate/cej

Development of a wideband microwave reactor with a coaxial cable structure

Tomohiko Mitani [a,c,*], Naoki Hasegawa [a,c], Ryo Nakajima [a,c], Naoki Shinohara [a,c], Yoshihiro Nozaki [b,c], Tsukasa Chikata [b,c], Takashi Watanabe [a,c]

[a] Research Institute for Sustainable Humanosphere, Kyoto University, Gokasho, Uji, Kyoto 611-0011, Japan
[b] Japan Chemical Engineering & Machinery Co. Ltd., 6-23 Kashima 4-chome, Yodogawa-ku, Osaka 532-0031, Japan
[c] CREST, JST, 4-1-8 Honcho, Kawaguchi, Saitama 332-0012, Japan

HIGHLIGHTS

- A wideband microwave reactor with a coaxial cable structure was designed.
- Insertion of a truncated cone-shaped PTFE device was used as a method to reduce microwave reflection.
- The reflection ratio was less than 2% for a 0.1 M NaOH solution.
- Microwave heating at 915 MHz, 1.7 GHz and 2.45 GHz was accomplished.

ARTICLE INFO

Article history:
Received 9 January 2016
Received in revised form 11 April 2016
Accepted 14 April 2016
Available online 21 April 2016

Keywords:
Microwave-assisted chemical reaction
Reactor
Wide frequency band
Coaxial cable structure
Electromagnetic simulation

ABSTRACT

A wideband microwave reactor with an output that includes the 915 MHz and 2.45 GHz ISM (Industrial, Scientific and Medical) bands was designed and fabricated. The reactor structure incorporated a coaxial cable, and a liquid sample was placed in the space between the inner and outer conductors. Insertion of a truncated cone-shaped polytetrafluoroethylene (PTFE) device was used as a method to reduce microwave reflection over a wide frequency range. The reactor had a volume of 360 ml and was designed employing a 3D electromagnetic simulation. Ultrapure water and a 0.1 M NaOH solution were selected as the liquid samples and experimentally measured permittivity data for these liquids were employed during the reactor simulations. The measured reflection ratio exhibited the same trend as the simulation results between 800 MHz and 2.7 GHz. The reflection ratio was especially low in the case of the NaOH solution (less than 2%), although this value increased to more than 40% upon removal of the PTFE insert. Microwave heating tests demonstrated that this reactor was able to heat liquid samples at 915 MHz, 1.7 GHz and 2.45 GHz, with estimated microwave absorption efficiencies varying between 28% and 66% depending on the frequency, sample type and heating duration. The reflection ratio and heating data demonstrated that this reactor functioned over a wide frequency range between 800 MHz and 2.7 GHz. A non-uniform temperature distribution in the sample remained a challenge that must be addressed in future work.

1. Introduction

Microwave-assisted chemical reactions have attracted significant attention over many years, primarily because the microwave heating mechanism, so-called dielectric heating, is quite different from conventional heating. One feature of this process is internal heating; microwaves propagate deeply into materials and thus simultaneously generate heat on both internal and external regions of the substance. Another feature is selective heating; microwaves preferentially heat materials having a large dielectric loss. Together, these mechanisms allow shorter heating durations and highly efficient chemical reactions. Indeed, previous studies have reported that microwave synthesis can reduce reaction times [1] and that microwave heating is more efficient than convective heating [2].

With respect to the microwave apparatus, 2.45 GHz and 915 MHz frequencies are used in most cases [1,3–9], for both regulatory and economic reasons. Worldwide, these frequencies have been allocated for the purposes of microwave heating and are

* Corresponding author at: Research Institute for Sustainable Humanosphere, Kyoto University, Gokasho, Uji, Kyoto 611-0011, Japan. Tel.: +81 774 38 3880; fax: +81 774 31 8463.
E-mail address: mitani@rish.kyoto-u.ac.jp (T. Mitani).

http://dx.doi.org/10.1016/j.cej.2016.04.064
1385-8947/

known as the ISM (Industrial, Scientific and Medical) bands. The prevalence of domestic microwave oven usage has led to a dramatic cost reduction in the case of high-power microwave units operating at 2.45 GHz.

The dielectric permittivity of a material is dependent on both frequency and temperature [10]. This implies that there may be an optimal frequency other than 2.45 GHz or 915 MHz that allows more effective microwave-assisted chemical reactions. On the laboratory scale, it is not necessary to use only the ISM bands due to the low levels of microwave power required to allow investigations of microwave-assisted reactions in small batches. However, there are currently no readily available units capable of generating microwaves in a number of frequency bands. In addition, the radiation type microwave reactors previously reported in the literature [6,9] are not suitable for wideband microwave irradiation because of the reactor frequency dependency that results from reflection, resonance and cutoff.

The objective of the present study was therefore to develop a wideband microwave reactor. For this purpose, we fabricated a coaxial cable structure, in which microwaves propagate in the transverse electromagnetic mode (TEM) with no cutoff frequency. In previous studies on microwave applicators [11] or radiators [12] using a coaxial cable, a liquid sample was irradiated with microwaves at the open end of the coaxial cable in the manner of dipole antenna-like radiation. In the present study, however, the microwaves were absorbed by a liquid sample based on propagation similar to that which occurs in a coaxial cable transmission line. This effect was obtained by positioning the liquid sample directly between the inner and outer conductors. In terms of the coaxial structure, a coaxial traveling microwave reactor (TMR) has been proposed to enable highly uniform microwave heating [13]. The TMR was designed via electromagnetic simulations only at 2.45 GHz; whereas the novelty of our designed reactor is realization of wideband microwave irradiation.

This wideband microwave reactor was designed using 3D electromagnetic simulations and had a target frequency range of 800 MHz to 2.7 GHz, a range that includes the ISM bands of 2.45 GHz and 915 MHz. Insertion of a truncated cone-shaped section of polytetrafluoroethylene (PTFE) device between the inner and outer conductors was used as a method to reduce microwave reflection over a wide frequency range. We verified the capabilities of the reactor, including the effectiveness of the PTFE insert, through electromagnetic simulations, microwave reflection measurements and microwave heating tests.

2. Materials and methods

2.1. Overview of the wideband microwave reactor

A cross-sectional schematic of the wideband microwave reactor along the axial direction is shown in Fig. 1. The reactor is rotationally symmetric along the central axis of the inner conductor. The outer and inner conductors produce the coaxial cable structure and a portion of a liquid sample is placed in the space between these conductors. A punched metal plate with 20 holes (each hole 6 mm in diameter) is mounted on the top surface of the liquid sample in order to prevent microwaves from leaking upwards through the sample and to avoid increases in the internal pressure of the reactor. An air release region above the plate buffers the inner pressure surge caused by sudden boiling. The inner and outer conductors, the metal plate and the wall of the air release area are all made of stainless steel (SUS 316L).

The microwave irradiation port consists of a commercially-available Type N connecter with a characteristic impedance of 50 Ω. A tapered section is inserted to smoothly connect the reactor

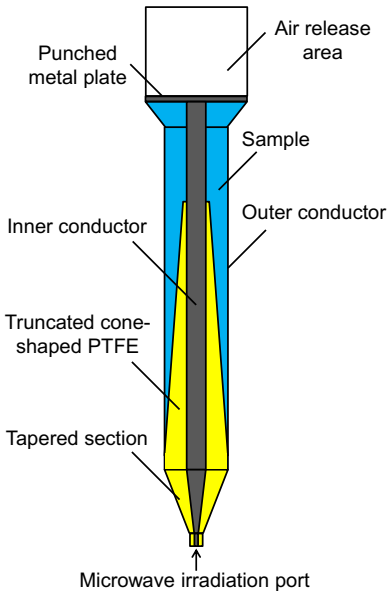

Fig. 1. A cross-sectional schematic of the wideband microwave reactor along the axial direction. The reactor is rotationally symmetric along the central axis of the inner conductor.

and the microwave irradiation port. The characteristic impedance was maintained at 50 Ω by adjusting the ratio of the diameters of the inner and outer conductors. The space between the conductors was filled with PTFE to prevent the liquid samples from flowing out at the tapered section.

The truncated cone-shaped PTFE insert plays a role of reducing microwave reflection over a wide frequency range. In the present study, we used aqueous samples, as described in Section 2.2. Since the relative permittivity of such samples is usually high, smooth microwave propagation is essential to reduce microwave reflections at the boundary surface between the tapered section and the liquid sample. In Section 4.1, we discuss the effectiveness of the PTFE insert.

2.2. Liquid samples

Two liquid samples were selected: ultrapure water (henceforth water) as a dielectric sample and 0.1 M NaOH (henceforth NaOH solution) as a dielectric and conductive sample. The water was obtained from an ultrapure water system (ELGA PURELAB Flex3 PF3XXXXM1) and had an electrical resistivity greater than 18 MΩ cm. The NaOH solution was obtained by dissolving NaOH (JIS Special Grade, Wako Pure Chemical Industries, Ltd.) in the same water.

2.3. Permittivity measurements of samples

The permittivity of the liquid sample is an important factor to consider when designing a microwave reactor. In general, permittivity is dependent on temperature and frequency [10]. For the reactor to be useful, the microwaves must penetrate into the liquid sample with minimal reflections at all frequencies and temperatures.

Permittivity measurements of the liquid samples were conducted using the coaxial probe method [14], which is a common means of assessing the dielectric properties of liquids [15,16]. A diagram of the permittivity measurement system is shown in Fig. 2. The liquid sample was placed in a glass bottle and subsequently both heated and stirred using a hot plate stirrer (AS ONE

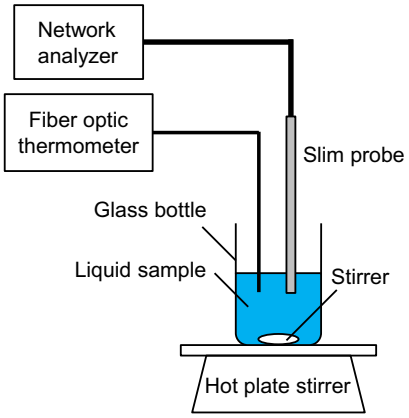

Fig. 2. A diagram of the permittivity measurement system.

DP-1S) while the sample temperature was monitored by a fiber optic thermometer (ANRITSU FL-2000). A slim dielectric probe (Agilent 85070E) was immersed in the sample and a network analyzer (Agilent N5242A) measured the reflection coefficient for the microwaves at the boundary between the probe and the sample, and the relative complex permittivity was then calculated over the frequency range from 500 MHz to 20 GHz. Permittivity measurements were repeated five times at temperatures of 30, 40, 50 and 60 °C.

2.4. Designing the wideband microwave reactor

The wideband microwave reactor was designed with the aid of the 3D electromagnetic simulation software package Femtet ver. 2015 (Murata Software). Femtet solves electromagnetic fields using the finite element method and calculates the reflection coefficient, S_{11}, for the input microwave port, defined as the element of the scattering matrix in a 1-port network circuit [17].

We simulated two types of reactors, as shown in Fig. 3. Fig. 3(a) presents our reactor design, in which the truncated cone-shaped PTFE piece is inserted (also shown in Fig. 1). Fig. 3(b) is a schematic of a reactor in which the PTFE part is not present. Although the latter reactor was not produced, we compared these two reactors by electromagnetic simulations to establish the effectiveness of the PTFE insert.

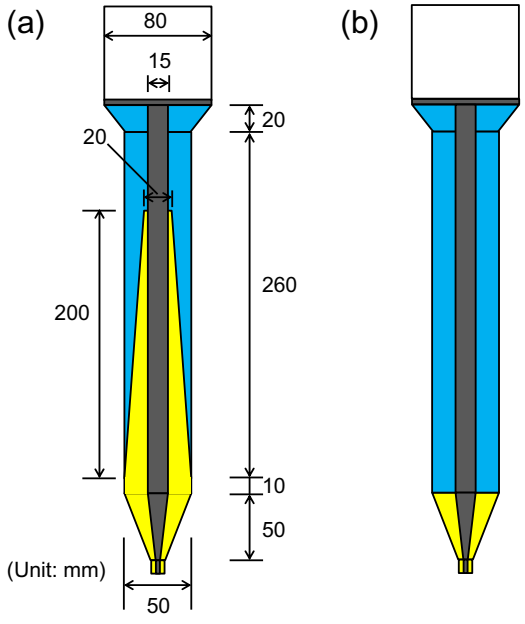

Fig. 3. Cross-sectional schematics of the two simulated microwave reactors: (a) with and (b) without the truncated cone-shaped PTFE insert. The reactors are rotationally symmetric along the central axis of the inner conductor.

The general simulation setup involved frequencies ranging from 800 MHz to 2.7 GHz with an input microwave power of 100 W. The values for the real part of the relative permittivity, the dielectric loss tangent and the density of the PTFE were 2.1, 0.002 and 2.16 kg/m^3, respectively. The conductivity and density of the SUS 316L were 1.35×10^6 S/m and 798 kg/m^3, respectively. The relative permittivity of water and the conductivity and relative permittivity of the NaOH solution were acquired from experimental data, as described in Section 3.1.

2.5. Microwave reflection measurements for the newly developed reactor

Microwave reflection measurements are an important aspect when investigating the reactor performance. A greater degree of microwave reflection leads to longer heating times and larger energy losses since less microwave energy penetrates into the sample.

A diagram of the microwave reflection measurement system is shown in Fig. 4. The reflection coefficient of the microwaves at the input port of the reactor, S_{11}, was measured using a network analyzer (Agilent N5242A). S_{11} is generally a complex number, and its absolute value, $|S_{11}|$, is less than or equal to 1. Here we introduce the reflection ratio, R, which is the ratio of the input power to the reflected power, as a means of intuitively understanding the applicator performance. R is calculated from the reflection coefficient by the following equation:

$$R = 100\% \cdot |S_{11}|^2. \quad (1)$$

A 360 mL aliquot of the test sample, either pure water or the NaOH solution, was poured into the reactor, at which point the liquid level reached the metal plate, as shown in Fig. 1. As the output power from the network analyzer was too weak to heat the sample, an electric heater was wound around the reactor as an alternative heating method. The sample temperature was measured using a multichannel fiber optic thermometer (ANRITSU FL-2400) at depths of 15, 10 and 5 cm from the metal plate, and these

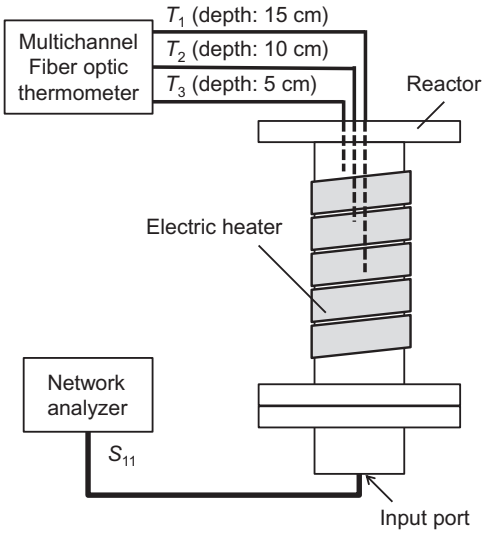

Fig. 4. A diagram of the microwave reflection measurement system.

temperatures are termed T_1, T_2 and T_3, respectively, as shown in Fig. 4. Microwave reflection measurements were executed at temperatures of 30, 40, 50 and 60 °C. A photographic image of the reactor is presented in Fig. 5.

2.6. Microwave heating trials

A diagram of the microwave heating test is shown in Fig. 6. Microwaves were generated using a signal generator (Agilent N5183A), amplified at 100 W by a semiconductor power amplifier (R&K GA0827-4754-R) and input to the reactor through the coaxial cable. The input power, P_i, and the reflected power, P_r, were monitored by a power meter (Agilent E4471A) through power sensors (Agilent N8485A). The sample temperatures T_1, T_2 and T_3 were measured in the same manner as described in Section 2.5. The values of P_i, P_r, T_1, T_2 and T_3 were logged at one second intervals using a data logger (GRAPHTEC GL220). In the present tests, the liquid sample was not stirred during the initial measurements of the temperature distribution in the reactor. For this reason, multipoint local temperature measurements were quite important for evaluating the microwave reactor because the local temperature in the liquid sample could be dependent on the measurement point during a microwave-assisted chemical reaction [2,18]. The duration of microwave irradiation was 5 min. The microwave heating tests were conducted three times each at frequencies of 915 MHz, 1.7 GHz and 2.45 GHz. The value of 1.7 GHz was selected since it represents an intermediate frequency between the ISM bands of 915 MHz and 2.45 GHz.

3. Results

3.1. Relative permittivity of liquid samples

Fig. 7 presents the relative permittivity results obtained from the pure water and the NaOH solution. The real and imaginary parts of the relative permittivity are plotted in Fig. 7(a) and (b), respectively. In the case of the pure water, the measured dielectric properties are well in accordance with the Debye model [10]. In the NaOH solution case, the real part of the relative permittivity exhibits almost the same trend as the pure water with regard to both frequency and temperature (Fig. 7(a)). In contrast, the imaginary part of the relative permittivity shows completely different trends, especially at lower frequencies.

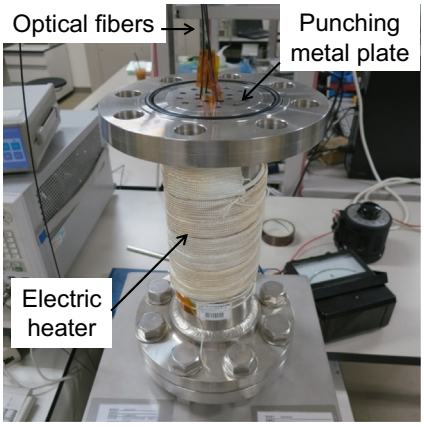

Fig. 5. A photograph of the newly developed microwave reactor. The electric heater was used to heat the reactor only during the microwave reflection measurements. The optical fibers were inserted in the reactor through the punched metal plate so as to measure the sample temperatures at depths of 15, 10 and 5 cm.

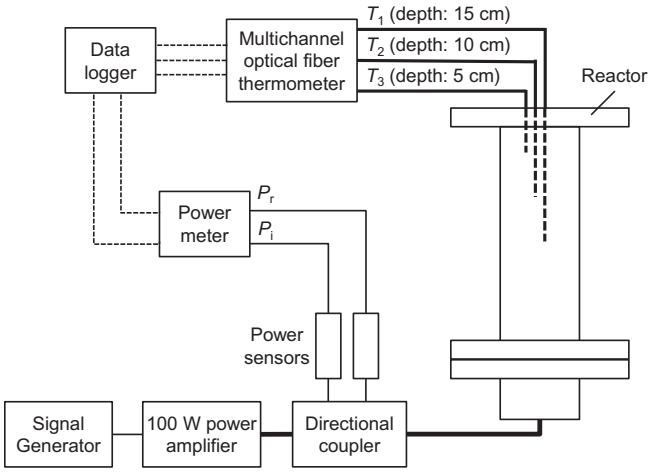

Fig. 6. A diagram of the microwave heating test apparatus.

The increase in the imaginary part of the relative permittivity for the NaOH solution with decreasing frequency is attributed to ion conduction. In the case of an ionic liquid, the measured values incorporate the conductivity, σ, in the imaginary part of the relative permittivity, ε'', as expressed in the following equation:

$$\varepsilon''_a = \varepsilon'' + \sigma/2\pi f\varepsilon_0, \quad (2)$$

where ε''_a is the imaginary part of the relative permittivity obtained from measurements, f is the frequency and ε_0 is the permittivity in vacuum. From Eq. (2), we can estimate σ by fitting the inverse proportional curve obtained in the low frequency range in which the effects of ε'' are negligible compared to those of σ. Table 1 shows the estimated conductivity at each temperature obtained from the experimental data. The conductivity of the NaOH solution is seen to increase with temperature.

3.2. Simulation and measurement results

Fig. 8 plots the simulated reflection ratios for the reactors shown in Fig. 3, using either water (Fig. 8(a)) or the NaOH solution (Fig. 8(b)) as samples. The values of the relative permittivity and conductivity shown here are imported from Fig. 7 and Table 1, respectively, for temperatures of 30, 40, 50 and 60 °C. In the case in which the PTFE insert shown in Fig. 3(b) is included, only the simulation results at 30 °C are shown.

Fig. 9 summarizes the experimental reflection ratio data obtained with the newly developed reactor with water (Fig. 9(a)) and the NaOH solution (Fig. 9(b)). Here we have replotted the simulation results at 30 and 60 °C from Fig. 8.

3.3. Microwave heating test results

Fig. 10 summarizes the temperature increases observed during microwave heating trials, employing water (Fig. 10(a)) or the NaOH solution (Fig. 10(b)). The temperature rise data indicate the differences between the measured temperatures at a given time and the temperatures prior to microwave irradiation. The plotted data show the averages of three measurement trials.

Fig. 11 shows the experimental results for the reflection ratio during the microwave heating tests. The reflection ratio, R, defined by Eq. (1) was calculated as the ratio between the measured input power, P_i, and reflected power, P_r, as follows:

$$R = 100\% \cdot P_r/P_i. \quad (3)$$

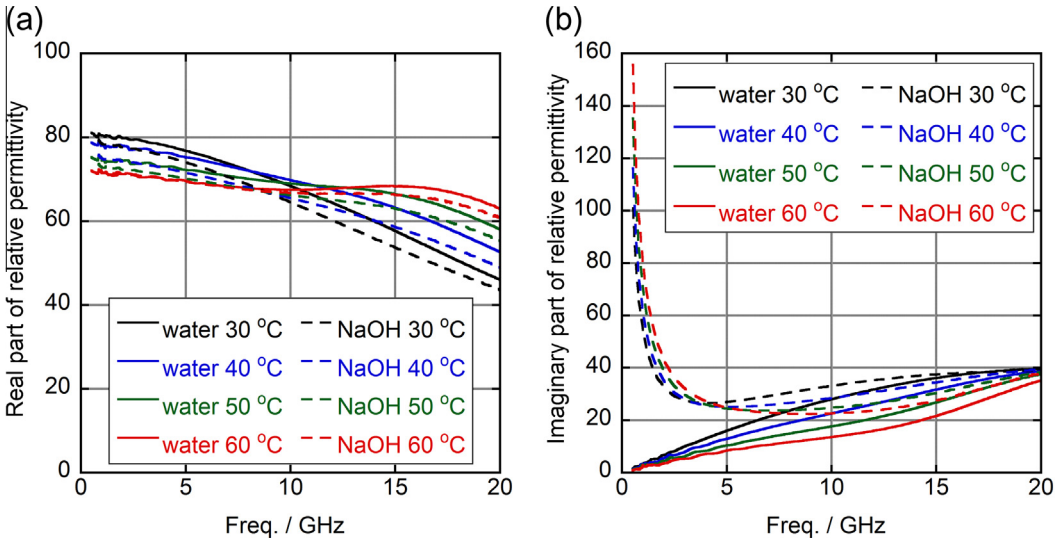

Fig. 7. Experimental results for the (a) real and (b) imaginary parts of the relative permittivity of the two different test liquids. The solid and dashed lines indicate the results for pure water and a NaOH solution, respectively. Note that the experimental data for the NaOH solution represent the apparent imaginary part of the relative permittivity because they include the conductivity of the solution.

Table 1
Estimated conductivity (σ) of a NaOH solution calculated from Eq. (2) and the experimental results from Fig. 7(a).

Temperature/°C	Estimated conductivity/(S/m)
30	2.65
40	3.12
50	3.69
60	4.28

4. Discussion

4.1. Effectiveness of the PTFE insert

The simulation results shown in Fig. 8 verify that the reflection ratio is drastically reduced by insertion of the truncated cone-shaped PTFE part. In general, radio waves will be reflected at a discontinuous boundary across the wave propagation direction. When the PTFE is removed, as shown in Fig. 3(b), reflection takes place at the discontinuous boundary between the tapered section and the liquid sample. The use of the PTFE part gradually changes the discontinuous boundary between the PTFE and the liquid sample in the wave propagation direction. Thus it is possible to mitigate reflection issues over a wide frequency range by this simple but effective method.

It should be noted, however, that this method is not a panacea for reducing reflections at all frequencies. As shown in Fig. 8(b), we observed a reflection ratio of more than 50% below 840 MHz when using water as the sample even when employing the PTFE. The effectiveness of this method is thus dependent on the microwave wavelength, the dielectric properties of the liquid sample and the reactor dimensions, including the height of the PTFE insert. When the wavelength is large compared to the reactor size, reflection gradually increases because the truncated cone shape appears as a discontinuous planar boundary.

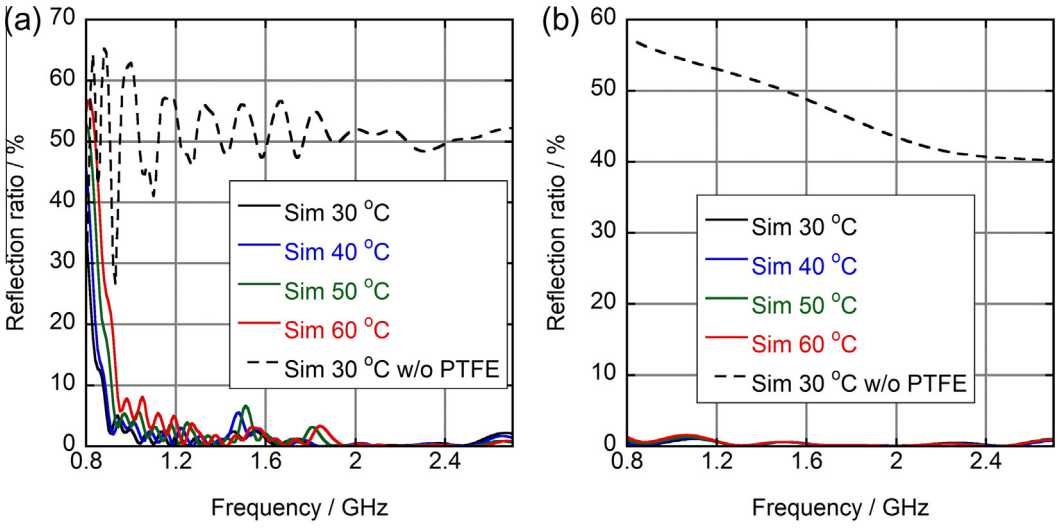

Fig. 8. Simulated reflection ratios for the reactors shown in Fig. 3, using liquid samples consisting of (a) pure water and (b) a NaOH solution. Relative permittivity and conductivity values were imported from Figs. 7 and 8 and Table 1 at each temperature. The legend "w/o PTFE" denotes the case in which the truncated cone-shaped PTFE insert shown in Fig. 3(b) was removed.

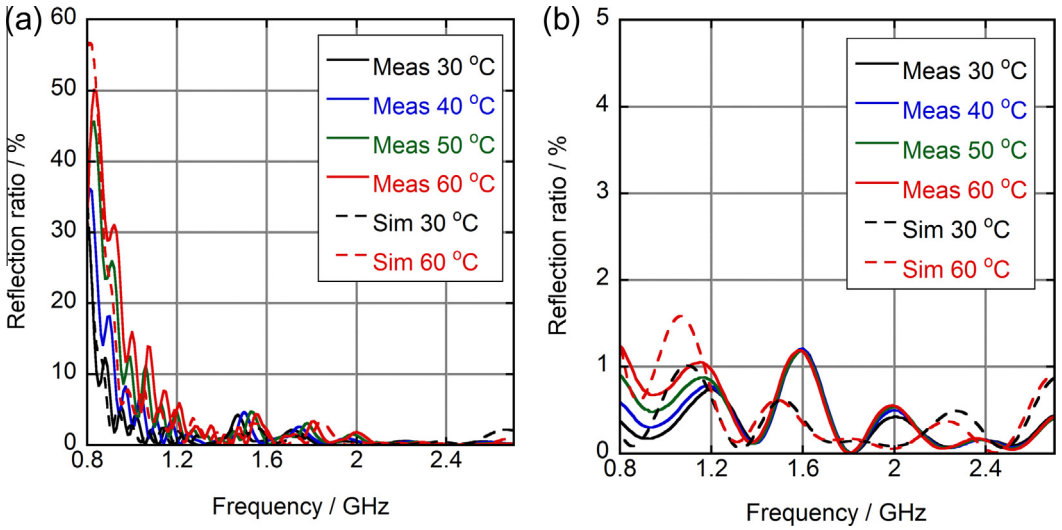

Fig. 9. Experimental reflection ratio data for the newly developed reactor, employing liquid samples consisting of (a) pure water and (b) a NaOH solution. The simulation results at 30 and 60 °C are replotted from Fig. 8.

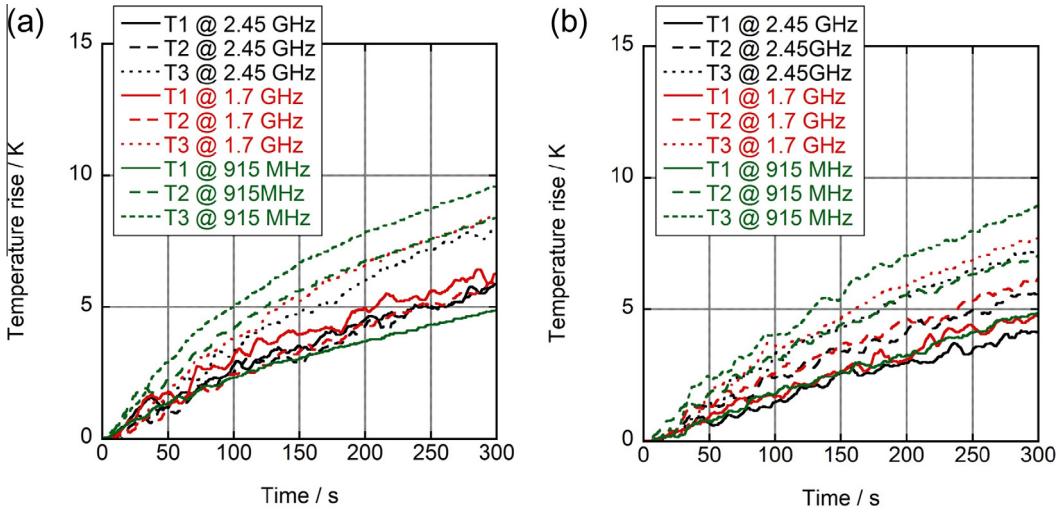

Fig. 10. Temperature rise using (a) pure water and (b) a NaOH solution during microwave heating trials. The measurement points at which T_1, T_2 and T_3 were acquired are described in Sections 2.5 and 2.6.

4.2. Availability of wideband microwave irradiation

Wideband microwave irradiation, which was the most important goal of the new reactor, was successfully achieved, as demonstrated by the data in Figs. 9–11. Although we conducted the heating trials at only three frequencies, the data verified that the microwaves propagate through the NaOH solution at any frequency from 800 MHz to 2.7 GHz with less than 2% reflection (Fig. 9(b)). The microwaves also propagate through the pure water at any frequency from 1.1 to 2.7 GHz with less than 10% reflection (Fig. 9(a)). The use of an additional device to reduce microwave reflection, such as an isolator, would allow use of the reactor at frequencies even lower than 1.1 GHz at the expense of some energy loss. The results for microwave heating of water at 915 MHz shown in Fig. 10(a) proves that heating proceeds efficiently even though some microwave power is reflected from the reactor.

One challenge with this reactor is a non-uniform temperature distribution in the liquid sample, as shown in Fig. 10. The greatest temperature difference recorded among the T_1, T_2 and T_3 values was 4.7 K after five minutes, in the case of water at 915 MHz. This temperature non-uniformity has to be addressed in future work to produce a reliable chemical reactor. Conventional stirring by a magnetic stirrer seems to be difficult to apply in this reactor as there is no rotational space on the bottom of the reactor. The metal punch plate will be replaced in future designs, allowing the sample to be instead agitated with a stirring rod.

4.3. Rough estimation of microwave absorption efficiency

We estimated the microwave absorption efficiency from the microwave heating data. The temperature distribution in the liquid sample was not uniform, as described in Section 4.2. Therefore, in the present paper, we take the experimental temperatures T_1, T_2 and T_3 as representative of the liquid sample. We also used specific heat and density values for the pure water and the NaOH solution of 4.2 J/g/K and 1 g/ml, respectively. Using these values, the microwave absorption efficiency, η, may be roughly estimated by the following equations:

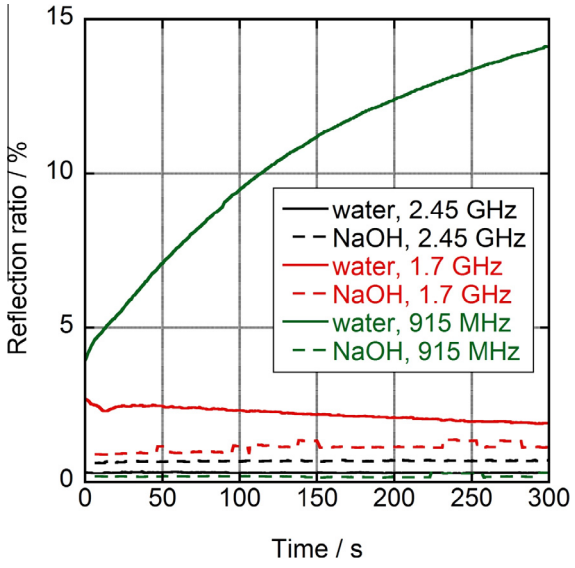

Fig. 11. Reflection ratios of the newly developed reactor during microwave heating trials. Ratio values equal the ratio between the measured input and reflected powers = P_r/P_i.

$$\eta = 100\% \cdot 360\text{g} \cdot 4.2\,\text{J/g/K} \cdot \{(\Delta T_1(t) + \Delta T_2(t) + \Delta T_3(t))/3\}/P_a(t), \quad (4)$$

$$\Delta T_n(t) = T_n(t) - T_n(t=0) \text{ and } (n = 1, 2, 3) \quad (5)$$

$$P_a(t) = \int_0^t (P_i - P_r)dt \quad (6)$$

where t is the duration of microwave irradiation, $P_a(t)$ is the integral of the available microwave power propagating into the reactor and $\Delta T_n(t)$ is the temperature rise obtained from Fig. 10.

Fig. 12 plots the estimated η values for the pure water and the NaOH solution at one minute intervals. It is evident that η reaches a maximum (66%) in the case of the water sample at 915 MHz, and a minimum (28%) in the case of the NaOH solution at 2.45 GHz. A larger η value was thus obtained with the water, and this parameter was also larger at lower frequencies.

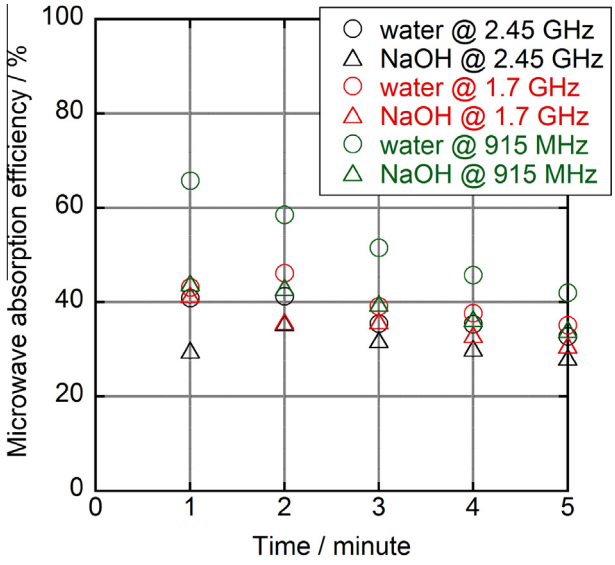

Fig. 12. Estimated microwave absorption efficiencies of the newly developed reactor during microwave heating trials.

The degradation of the microwave absorption efficiency is attributed to two main factors: thermal dissipation from the reactor and the coarseness of the temperature measurements. As shown in Figs. 10 and 12, the temperature rise gradually plateaus and η is reduced as the microwave irradiation time is extended. In the present experiments, the reactor was not thermally insulated and was exposed to the surrounding air, as shown in Fig. 5. Hence thermal insulation or external heating would increase the efficiency of the reactor. With respect to temperature measurements, the deepest measurement point was 15 cm even though the liquid sample had a depth of 28 cm, as shown in Fig. 3. The sample temperature might therefore be higher at a greater depth since the microwaves were absorbed by the sample starting from the input port.

5. Conclusions

A wideband microwave reactor with a coaxial cable structure was designed via 3D electromagnetic simulation. This reactor, which generates frequencies including the two ISM bands at 915 MHz and 2.45 GHz, will enable the investigation of microwave-assisted chemical reactions at various frequencies without the need to modify the reactor. Furthermore, this device permits varying of the microwave frequency over a certain range even during chemical reactions. Although the evident non-uniform temperatures in sample solutions is a challenging problem that must be addressed in future work, the newly developed reactor is anticipated to allow a wide variety of microwave-assisted chemical reactions to be examined for the first time ever.

Acknowledgements

This work was supported by CREST, JST. Measurements of the reflection ratios and the microwave heating tests were conducted through a collaborative research program: the Analysis and Development System for Advanced Materials (ADAM) at the Research Institute for Sustainable Humanosphere, Kyoto University.

References

[1] C. Oliver Kappe, Microwave dielectric heating in synthetic organic chemistry, Chem. Soc. Rev. 37 (2008) 1127–1139.
[2] R. Cherbański, Calculation of critical efficiency factors of microwave energy conversion into heat, Chem. Eng. Technol. 34 (2011) 2083–2090.
[3] S. Li, G. Zhang, P. Wang, H. Zheng, Y. Zheng, Microwave-enhanced Mn-Fenton process for the removal of BPA in water, Chem. Eng. J. 294 (2016) 371–379.
[4] Z. Xiong, C. Wu, Q. Hu, Y. Wang, J. Jin, C. Lu, et al., Promotional effect of microwave hydrothermal treatment on the low-temperature NH3-SCR activity over iron-based catalyst, Chem. Eng. J. 286 (2016) 459–466.
[5] H. Zhou, L. Hu, J. Wan, R. Yang, X. Yu, H. Li, et al., Microwave-enhanced catalytic degradation of p-nitrophenol in soil using $MgFe_2O_4$, Chem. Eng. J. 284 (2016) 54–60.
[6] N. Wang, P. Wang, Study and application status of microwave in organic wastewater treatment – a review, Chem. Eng. J. 283 (2016) 193–214.
[7] E. Gjuraj, R. Kongoli, G. Shore, Combination of flow reactors with microwave-assisted synthesis: smart engineering concept for steering synthetic chemistry on the "fast lane", Chem. Biochem. Eng. Q. 26 (2012) 285–307.
[8] R. Cherbański, E. Molga, Intensification of desorption processes by use of microwaves-An overview of possible applications and industrial perspectives, Chem. Eng. Process. Process Intensif. 48 (2009) 48–58.
[9] T.N. Glasnov, C.O. Kappe, Microwave-assisted synthesis under continuous-flow conditions, Macromol. Rapid Commun. 28 (2007) 395–410.
[10] V.V. Komarov, Handbook of Dielectric and Thermal Properties of Materials at Microwave Frequencies, Artech House, 2012.
[11] I. Longo, A.S. Ricci, Chemical activation using an open-end coaxial applicator, J. Microw. Power Electromagn. Energy 41 (2007) 4–19.
[12] G.B. Gentili, M. Linari, I. Longo, A.S. Ricci, A coaxial microwave applicator for direct heating of liquids filling chemical reactors, IEEE Trans. Microw. Theory Tech. 57 (2009) 2268–2275.

[13] G.S.J. Sturm, M.D. Verweij, A.I. Stankiewicz, G.D. Stefanidis, Microwaves and microreactors: design challenges and remedies, Chem. Eng. J. 243 (2014) 147–158.
[14] D.V. Blackham, R.D. Pollard, An improved technique for permittivity measurements using a coaxial probe, IEEE Trans. Instrum. Meas. 46 (1997) 1093–1099.
[15] S. Tsubaki, M. Hiraoka, S. Hadano, H. Nishimura, K. Kashimura, T. Mitani, Functional group dependent dielectric properties of sulfated hydrocolloids extracted from green macroalgal biomass, Carbohydr. Polym. 107 (2014) 192–197.
[16] S. Horikoshi, S. Matsuzaki, T. Mitani, N. Serpone, Microwave frequency effects on dielectric properties of some common solvents and on microwave-assisted syntheses: 2-allylphenol and the C12–C2–C12 Gemini surfactant, Radiat. Phys. Chem. 81 (2012) 1885–1895.
[17] D.M. Pozer, Microwave Engineering, fourth ed., John Wiley & Sons Inc., 2012.
[18] M.A. Herrero, J.M. Kremsner, C.O. Kappe, Nonthermal microwave effects revisited: on the importance of internal temperature monitoring and agitation in microwave chemistry, J. Org. Chem. 73 (2008) 36–47.